Performance-Oriented Coordinated Adaptive Robust Control for Four-Wheel Independently Driven Skid Steer Mobile Robot

Article *in* IEEE Access · September 2017

DOI: 10.1109/ACCESS.2017.2754647

CITATIONS
23

READS
545

3 authors:

Jianfeng Liao
Zhejiang University
10 PUBLICATIONS **79** CITATIONS

SEE PROFILE

Zheng Chen
Zhejiang University
88 PUBLICATIONS **1,731** CITATIONS

SEE PROFILE

Bin Yao
Purdue University
344 PUBLICATIONS **10,133** CITATIONS

SEE PROFILE

This article has been accepted for publication in a future issue of this journal, but has not been fully edited. Content may change prior to final publication. Citation information: DOI 10.1109/ACCESS.2017.2754647, IEEE Access

Performance-Oriented Coordinated Adaptive Robust Control for Four-Wheel Independently Driven Skid Steer Mobile Robot

Jianfeng Liao, Zheng Chen and Bin Yao, *Senior Member, IEEE*,

***Abstract*—Four-wheel independently driven skid-steered mobile robots are widely used in the fields of industrial automation and outdoor exploration. In most of existing controllers of skid-steered mobile robots, the wheel velocities are controlled independently to track the desired velocities from the high level kinematic controller. However, this kind of control method may lead to chattering phenomenon of skid-steered mobile robots in practice, when the desired velocity commands of four wheels are not matched under different ground conditions. In this paper, the coordinated control problem is investigated for the four-wheel independently driven skid steer mobile robots, so as to solve the chattering phenomenon and also achieve good control performance under different ground conditions. Since the mobile robots are over-actuated and lack of suspension systems, a coordinated adaptive robust control scheme integrated with torque allocation technique is proposed. First, an adaptive robust control law is developed to attenuate the negative effects of load variations and uncertainties. Second, instead of directly giving the desired velocity commands, a torque control and allocation algorithm is developed to regulate the driving torque of each wheel motor. A coordinated control law with considering the wheel slip compensation is also proposed. Comparative experiments are carried out, and the results show the proposed scheme can avoid the chattering problem and achieve the excellent performance under different ground conditions.**

***Index Terms*—Mobile robot, skid steer, coordinated control, adaptive control, control allocation.**

I. Introduction

Skid-steered mobile robots are widely applied in the fields of industrial automation and outdoor exploration. The schematic of a skid-steered four-wheel independently driven mobile robot is shown in Fig.1. Since the lack of a steering system, the skid steer mobile robots have the advantage of outdoor task[1], [2], [3]. However, the mechanical structure and the varying wheel/ground interactions will also lead to the complexity of dynamic modeling and good controller design. Furthermore, to improve the driving ability based on the practical requirements, the skid steer mobile robot considered in this paper is four-wheel independently driven. At present, a large number of papers have investigated on the trajectory tracking control of two wheel mobile robots. However, seldom publications pay attention to four-wheel independently driven skid-steered mobile robots.

Generally, the controller for mobile robots can be summarized into two classes: kinematic controller(the control command for the mobile robots is the driving wheel velocities) and dynamic controller(the control command is the driving torques)[4], [5], [6], [7], [8]. The kinematic control is the most widely used in actually application[9], [10], [11], which does not consider the skidding of the robot wheels. To achieve a better performance, several approaches have been proposed to address this slip problem with the robot's dynamics[7], [12], but they will also increase the complexity of controller design. Furthermore, in the above control researches of wheeled mobile robots, the ground and wheels interactions are not taken into consideration. But in most real applications, due to uneven ground, or slippery terrain conditions, the interactions can't be ignored [7], [13]. As a result, the controllers designed with a no-slip model, may not work properly. For skid-steered mobile robots, since lack of the steering system, differential velocities between the two sized are applied to achieve steering requirement which will easily lead to lateral skidding of the wheels for the kinematic control. In the other side, the inevitable uncertainties in the mobile robot's dynamics will also take important effects on the performance of mobile robots, which becomes another challenging issue for the control design. Recently, a great deal of control methods have been proposed to handle the model uncertainties, such as adaptive control[1], [14], neural network[15], [16] and robust control[7], [17], [18]. Moreover, Yao and Tomizuka developed the adaptive robust control (ARC) to deal with both parameter and model uncertainties together in one controller, and subsequently verified through various application studies with comparative experimental results[19], [20], [21], [22]. With these ARC controllers, the specified tracking transient performance can be achieved and final tracking accuracy in general is guaranteed. And thus could be the good guidance for the dynamic controller design of skid-steer mobile robots.

Another problem should be noted that the skid-steered mobile robot considered in this paper is four-wheel independently driven, which means the robot is an over-actuated system. In the present work, the wheels on the each side are often supposed to rotate at the same speed. To guarantee this condition, two methods are usually used: a) the wheels

Jianfeng Liao, Zheng Chen and Bin Yao are with the State Key Laboratory of Fluid Power and Mechatronic Systems, Zhejiang University, Hangzhou 310027, China. Zheng Chen is also with the Ocean College, Zhejiang University, 310027 Hangzhou, China. Bin Yao is also with the School of Mechanical Engineering, Purdue University, West Lafayette, IN 47907 USA.

Corresponding author: Zheng Chen (email: zheng_chen@zju.edu.cn)

The work is supported by the National Natural Science Foundation of China (No.61603332), the Science Fund for Creative Research Groups of National Natural Science Foundation (No.51521064), Youth Funds of the State Key Laboratory of Fluid Power and Mechatronic Systems (Zhejiang University), and the Fundamental Research Funds for the Central Universities (No.2016QNA4038).

This article has been accepted for publication in a future issue of this journal, but has not been fully edited. Content may change prior to final publication. Citation information: DOI 10.1109/ACCESS.2017.2754647, IEEE Access

on each side is mechanically connected together, and the controller design is not much difference with the two wheel mobile robot[23], [24]; b) the wheels are regulated with velocity controller, where the controller design is similar with the kinematic control[11]. However, it can't be ignored that there are fundamental differences between the four-wheel independently driven mobile robot in this paper and the above two situations. Thus, to achieve a better performance, the driving torque allocation becomes an possible solution for this problem. Some control allocation techniques are proposed in [25], [26] for over-actuated ground vehicle, where the diving torques are directly distributed based on the energy consumption. However, since the skid-steered mobile robot in this paper isn't equipped with steer system and suspension system, the control design for it is much different from the ground vehicle and the chattering phenomenon is found in practice with the traditional controller. Thus, for the skid-steered mobile robot, the appropriate control strategies are needed to take into account the wheel/ground interactions and four-wheel driven characteristics.

In this paper, for skid-steered four-wheel independently driven mobile robot, a control oriented kinematic and dynamic model is first presented. Furthermore, a coordinated adaptive robust control(ARC) integrated with the torque allocation technique is proposed to track the desired motion trajectory. The adaptive robust control [27], [21], [22] is developed to attenuate the negative effects of load variations and uncertainties. And the proposed control strategy also addresses the over-actuated scheme with the control allocation[28], [29] to regulate the driving torques, whose excellent performance has also been verified in [30], [31]. Thus, with this kind of controller design, the tracking performance can be improved and the chattering problem for skid-steered mobile robot can be avoided.

This paper is organized as follows. In section II, the control oriented dynamic model of a four-wheel independently driven skid steered mobile robot is developed. Section III presents an adaptive robust trajectory controller design for the skid-steered mobile robot and the proposed torque allocation technique with driving torque/wheel slip coordination. Experimental results on a skid-steered mobile robot are compared in section IV. Finally, we conclude the paper in section V.

II. System Dynamics and Problem formulation

A. Kinematic and dynamic model

The mobile robot investigated in this paper is shown in Fig.1, which is driven with four independently wheels. The rotation of the mobile robot is achieved from different wheel velocities on each side, due to the absence of steering system. To obtain a better outdoor exploration, the wheels and body are connected directly. The reference coordinate system is named as OXY. The body fixed coordinate system $o_r x_r y_r$ is attached on the mobile robot, where o_r is the origin of the body fixed coordinate system, which locates at the middle between the driving wheels. G is the mass center of the skid steered mobile robot. $2w$ is the width between the driving wheels. l_f and l_r are the distances from the center of mass to the front and rear wheel axles, respectively. With the defined references, the pose of the robot is represented by

$$\mathbf{q} = (x, y, \phi)^T \tag{1}$$

where (x, y) is the coordinate of o_r with respect to reference coordinate system, and ϕ is the rotation angle.

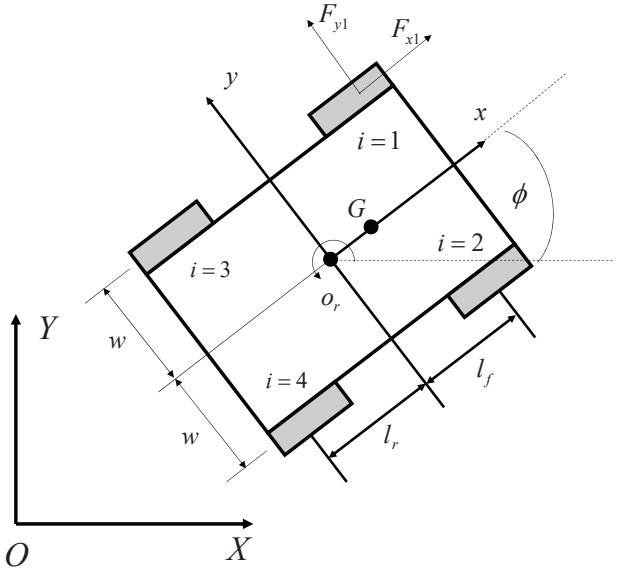

Fig. 1. Four-wheel independently driven skid steered mobile robot

The kinematic model of a four-wheeled independently driven skid-steered mobile robot can be expressed as[1]

$$\dot{\mathbf{q}} = \mathbf{S}(\mathbf{q})\mathbf{v} + \mathbf{A}(\mathbf{q})v_y \tag{2}$$

where $\mathbf{v} = [v_x, \omega]$ represents the linear and angular velocity of the robot; v_y is the lateral velocity of the robot; the $\mathbf{S}(\mathbf{q})$ and $\mathbf{A}(\mathbf{q})$ are defined as

$$\mathbf{S}(\mathbf{q}) = \begin{bmatrix} cos(\phi) & 0 \\ sin(\phi) & 0 \\ 0 & 1 \end{bmatrix}, \mathbf{A}(\mathbf{q}) = \begin{bmatrix} -sin(\phi) \\ cos(\phi) \\ 0 \end{bmatrix} \tag{3}$$

From the figure1, we can find that the frictions between the wheels and ground result in the motion of mobile robot. The friction forces acting on the mobile robot is presented in Fig.1. Thus, with Newton's second law, the dynamic model of the mobile robot system can be described as

$$\begin{aligned} &m(\dot{v_x} - v_y\omega) = F_{x1} + F_{x2} + F_{x3} + F_{x4} + d_x \\ &m(\dot{v_y} + v_x\omega) = F_{y1} + F_{y2} + F_{y3} + F_{y4} + d_y \\ &J\dot{\omega} = -wF_{x1} + l_f F_{y1} + wF_{x2} + l_f F_{y2} \\ &-wF_{x3} - l_r F_{y3} + wF_{x4} - l_r F_{y4} + d_\phi \end{aligned} \tag{4}$$

where m and J are the robot mass and inertia about the yaw axis. $F_{xi}, i = 1, 2, 3, 4$, $F_{yi}, i = 1, 2, 3, 4$ are the friction forces acting on the mobile robot. d_x, d_y, d_ϕ represent disturbances. w is the width of mobile robot. Referring to the equation $\mathbf{v} = [v_x, \omega]^T$, the dynamics(4) can be rewritten as

$$\begin{aligned} &\mathbf{M}\dot{\mathbf{v}} + \mathbf{A}_1 v_y = \mathbf{u} + \mathbf{d} \\ &m(\dot{v_y} + v_x\omega) = u_y + d_y \end{aligned} \tag{5}$$

where the $\mathbf{M} = diag[m, J]$ is diagonal inertia matrix, respectively; $\mathbf{A}_1$ is defined as $[-m\omega, 0]^T$; $\mathbf{u} = [u_x, u_\phi]^T$ denotes

This article has been accepted for publication in a future issue of this journal, but has not been fully edited. Content may change prior to final publication. Citation information: DOI 10.1109/ACCESS.2017.2754647, IEEE Access

the driving forces, where $u_x = F_{x1} + F_{x2} + F_{x3} + F_{x4}$ is the sum of forces acting on the mobile robot along the longitudinal direction and $u_\phi = -wF_{x1} + l_f F_{y1} + wF_{x2} + l_f F_{y2} - wF_{x3} - l_r F_{y3} + wF_{x4} - l_r F_{y4}$ is the sum of moments acting on the mobile robot. The second term of equation(5) represents the lateral slip motion. $u_y = F_{y1} + F_{y2} + F_{y3} + F_{y4}$ is the sum of friction forces acting on the robot along the lateral direction; $\mathbf{d} = [d_x, d_\phi]^T$ is the nominal value of the lumped modeling uncertainty and disturbance

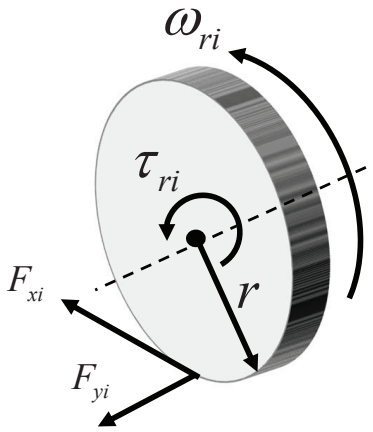

Fig. 2. Wheel rotation motion

Referred to the dynamic(5), the driving forces are the result of the interactions between tires and road. From Fig.2, we can obtain the dynamics of driving wheels

$$J_{ri}\dot{\omega}_{ri} + c_{ri}\omega_{ri} + f_{ri} = \tau_{ri} - rF_{xi} + d_{ri}, i = 1, 2, 3, 4 \quad (6)$$

where J_{ri} inertia of wheel; ω_{ri} denotes the angular velocity of wheel; c_{ri} represents the viscous friction constant of wheel; $f_{ri}(\dot{q})$ is the Coulomb friction of the motor and reducer modeled by $f_{ri} = A_{fi}S_f(\dot{q})$, where A_{fi} is the Coulomb friction coefficient and $S_f(\dot{q})$ is a known approximate function of the traditional discontinuous sign function $sgn(\dot{q})$ that is used to compensate friction in implementation; τ_{ri} denotes the motor torque; d_{ri} is the disturbance; r is the radius of wheel.

B. Error dynamics

To design a controller with such system(5)(6), we apply the output redefinition technique[32]. The new output equations are given by

$$\mathbf{z} = \begin{bmatrix} z_1 \\ z_2 \end{bmatrix} = \begin{bmatrix} x + Lcos(\phi) \\ y + Lsin(\phi) \end{bmatrix} \quad (7)$$

where L is chosen as a positive constant. Differentiating the equation (7), we can obtain the new dynamics as

$$\dot{\mathbf{z}} = \mathbf{T}\mathbf{v} + \mathbf{A_2}\mathbf{v_y} + \mathbf{d_k} + \tilde{\mathbf{d}}_\mathbf{k} \quad (8)$$

where $\mathbf{T}$ and $\mathbf{A}_2$ are defined as

$$\mathbf{T} = \begin{bmatrix} cos(\phi) & -Lsin(\phi) \\ sin(\phi) & Lcos(\phi) \end{bmatrix}, \mathbf{A}_2 = \begin{bmatrix} sin\phi \\ -cos\phi \end{bmatrix} \quad (9)$$

Referring to equation (4), taking the second time-derivative of (7), the following dynamics is derived.

$$\mathbf{M}_t\ddot{\mathbf{z}} + \mathbf{C}_t\dot{\mathbf{z}} = \mathbf{u}_t + \mathbf{d}_t + \mathbf{A}_t + \tilde{\mathbf{\Delta}}_t \quad (10)$$

where

$$\begin{aligned} &\mathbf{M}_t = \mathbf{T}\mathbf{M}\mathbf{T}^{-1}, \mathbf{C}_t = \mathbf{T}\mathbf{M}\dot{\mathbf{T}}^{-1}, \mathbf{u}_t = \mathbf{T}\mathbf{u}, \\ &\mathbf{A}_t = [-m\omega v_y, J/L\dot{v}_y]^T, \mathbf{d}_t = \mathbf{T}\mathbf{d}, \tilde{\mathbf{\Delta}}_t = \mathbf{T}\tilde{\mathbf{\Delta}} \end{aligned} \quad (11)$$

Let the trajectory tracking error vector as $\mathbf{e} = [e_x, e_y]^T = [z_1(t) - x_d(t), z_2(t) - y_d(t)]$, where $\mathbf{z}_d(t) = [x_d(t), y_d(t)]$ is the reference trajectory. Then the system error dynamics can be derived as

$$\begin{aligned} &\dot{\mathbf{e}} + \mathbf{z_d} = \mathbf{T}\mathbf{v} + \mathbf{A_2}\mathbf{v_y} + \mathbf{d_k} + \tilde{\mathbf{d}}_\mathbf{k} \\ &\mathbf{M}_t\ddot{\mathbf{e}} + \mathbf{C}_t\dot{\mathbf{e}} + \mathbf{M}_t\ddot{\mathbf{z}}_d + \mathbf{C}_t\dot{\mathbf{z}}_d + \mathbf{B}_t\dot{\mathbf{z}}_d + \mathbf{A}_t \\ &= \mathbf{u}_t + \mathbf{d}_t + \tilde{\mathbf{\Delta}}_t \end{aligned} \quad (12)$$

It is well known (12) has the following properties

Property 1. *The $\boldsymbol{M}_t$ is symmetric and positive definite.*

Property 2. *The matrix $\boldsymbol{M}_t - 2\boldsymbol{C}_t$ is skew-symmetric.*

The matrices or vectors in (12), namely, $\mathbf{d}_k$, $\mathbf{M}_t$, $\mathbf{C}_t$, $\mathbf{d}_t$, $\mathbf{A}_t$ can be written as linear regression form described by a set of parameters defined by $\boldsymbol{\theta} = [\boldsymbol{\theta}_k^T, \boldsymbol{\theta}_d^T]^T = [\theta_1, \theta_2, ..., \theta_8]^T = [d_{kx}, d_{k\phi}, m, J, d_{nx}, d_{n\phi}, A_{t1}, A_{t2}]^T$. In general, due to various reasons such as the change of payloads, the parameter vector $\boldsymbol{\theta}$ cannot be exactly known . However, the extent of the parameters can be roughly known in advance. Therefore, the following assumptions are made[7], [33]

Assumption 1. *We assume that the slip velocity v_y and its derivative $\|\dot{v}_y\|$ are bounded.*

Assumption 2. *The extent of the parameters and uncertain nonlinearities are known, i.e.,*

$$\boldsymbol{\theta} \in \Omega \triangleq \{\boldsymbol{\theta} : \boldsymbol{\theta}_{min} \leq \boldsymbol{\theta} \leq \boldsymbol{\theta}_{max}\} \quad (13)$$

$$\tilde{\boldsymbol{d}} \in \triangleq \{\boldsymbol{d} : |\tilde{\boldsymbol{d}}| \leq \delta_{\boldsymbol{d}}\} \quad (14)$$

where $\boldsymbol{\theta}_{min} = [\theta_{1min}, \theta_{2min}, ..., \theta_{8min}]^T$, $\boldsymbol{\theta}_{max} = [\theta_{1max}, \theta_{2max}, ..., \theta_{8max}]^T$ and $\boldsymbol{\delta}_d$ are known.

C. Problem formulation

With the the mathematical model for the motion of the skid steer mobile robot(12),(6), the following performance requirements would like to be considered in the controller design

1) Tracking performance: the controller is synthesized to track the reference trajectory as well as possible in the presence of uncertainties.

2) Motor torque allocation: With the traditional controller, the unexpected chattering phenomenon may happen, which would lead to damage of the mechanical components. Thus, the motor torque should be properly allocated.

Based on these statements, for skid steer mobile robot, the objective of controller design is to synthesize control inputs τ_{ri} in the presence of uncertainties and disturbances, such that the motor toque can be properly coordinated and the robot can track the desired trajectory.

This article has been accepted for publication in a future issue of this journal, but has not been fully edited. Content may change prior to final publication. Citation information: DOI 10.1109/ACCESS.2017.2754647, IEEE Access

III. CONTROL ALGORITHM

A. Overall control structure

Based on the aforementioned analysis and problem statements, our controller was proposed to achieve stable tracking of the desired trajectory for over-actuated skid steer mobile robot. To deal with this kind of problem, a coordinated control structure consisting of a adaptive robust control(ARC control law and wheel torque allocation) and a motion compensation scheme(kinematic control and linear feedback) is proposed to track the desired trajectory, as shown in Fig.3. Since the model

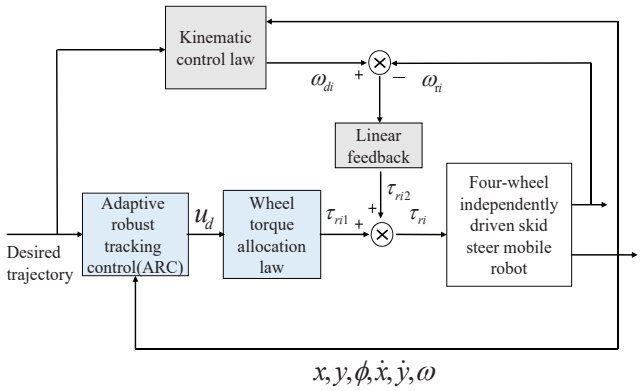

Fig. 3. Overall control structure

(5) cannot fully describe the actual parameter uncertainties and robot dynamics. Thus, the ARC is incorporated such that the uncertainties in mobile robot dynamics can be attenuated. The ARC controller offers the total forces/moments(virtual control inputs) needed to track the desired mobile robot trajectory. For the control allocation part, with the given the virtual control inputs, the actuator redundancy is resolved in real time to implement the command on the individual actuators. Moreover, kinematic controller offers desired wheel velocities that aims to coordinate the motion of the wheels. The design of the controller will be given later and experiments are carried out to verify the proposed control law.

B. Discontinuous Projection

The adaptation law with discontinuous projection can be given by[19]:

$$\dot{\hat{\boldsymbol{\theta}}} = Proj_{\hat{\boldsymbol{\theta}}}(\boldsymbol{\Gamma}\boldsymbol{\eta}) \tag{15}$$

where $\hat{\boldsymbol{\theta}}$ denotes the on-line estimate of $\boldsymbol{\theta}$ and $\tilde{\boldsymbol{\theta}} = \hat{\boldsymbol{\theta}} - \boldsymbol{\theta}$ represents the parameter estimation error. $\boldsymbol{\Gamma} > 0$ is symmetric positive definite and $\boldsymbol{\eta}$ is an adaptation function to be given later. The projection mapping $Proj_{\hat{\boldsymbol{\theta}}}(\bullet) = [Proj_{\hat{\boldsymbol{\theta}}}(\bullet_1), ..., Proj_{\hat{\boldsymbol{\theta}}}(\bullet_3)]$ is defined in [19] as

$$Proj_{\hat{\boldsymbol{\theta}}_i}(\bullet_i) = \begin{cases} 0, & if \quad \hat{\theta}_i = \theta_{imax} \quad and \quad \bullet_i > 0 \\ 0, & if \quad \hat{\theta}_i = \theta_{imin} \quad and \quad \bullet_i < 0 \\ \bullet_i, & otherwise \end{cases} \tag{16}$$

The projection mapping used in (16) has the following properties.

$$\mathbf{P1}) \quad \boldsymbol{\theta} \in \boldsymbol{\Omega} \triangleq \{\boldsymbol{\theta} : \boldsymbol{\theta}_{min} \leq \boldsymbol{\theta} \leq \boldsymbol{\theta}_{max}\} \tag{17}$$

$$\mathbf{P2}) \quad \tilde{\boldsymbol{\theta}}(\boldsymbol{\Gamma}^{-1} Proj_{\hat{\boldsymbol{\theta}}}(\boldsymbol{\Gamma}\boldsymbol{\eta}) - \boldsymbol{\eta}) \leq 0, \forall \boldsymbol{\eta} \tag{18}$$

C. Kinematic control law

In this section, the most used kinematic control law is introduced. The kinematic model(12) can be linearly parameterized as

$$\dot{\mathbf{e}} + \mathbf{z_d} = \mathbf{T}\mathbf{v} + \mathbf{A_2}\mathbf{v_y} + \boldsymbol{\Psi}_\mathbf{k}(\mathbf{z}, \dot{\mathbf{z}}, \mathbf{t})\boldsymbol{\theta} + \tilde{\mathbf{d}}_\mathbf{k} \tag{19}$$

where $\mathbf{d}_k = \boldsymbol{\Psi}_k(\mathbf{z}, \dot{\mathbf{z}}, \mathbf{t})\boldsymbol{\theta}$, $\boldsymbol{\Psi}_k \in R^{2\times 10}$ matrix is a known functions. With the error dynamic(19), choose the ARC law[34], [35] as

$$\begin{aligned} &\mathbf{v}_d = \mathbf{T}^{-1}\mathbf{u}_v, \mathbf{u}_v = \mathbf{u}_{va} + \mathbf{u}_{vs}, \\ &\mathbf{u}_a = \mathbf{z_d} - \mathbf{A_2}\mathbf{v_y} + \boldsymbol{\Psi}_\mathbf{k}(\mathbf{z}, \dot{\mathbf{z}}, \mathbf{t})\hat{\boldsymbol{\theta}} \end{aligned} \tag{20}$$

where the model compensation term $\mathbf{u}_v = \mathbf{T}\mathbf{v}$, $\mathbf{u}_{va}$ is designed to track a trajectory perfectly, and the robust control law $\mathbf{u}_{vs}$ consists of two terms

$$\mathbf{u}_{vs} = \mathbf{u}_{vs1} + \mathbf{u}_{vs2}, \ \mathbf{u}_{vs1} = -\mathbf{K}_k\mathbf{e} \tag{21}$$

where $\mathbf{u}_{vs1}$ is a simple linear feedback term and $\mathbf{K}_k$ is a symmetric positive definite matrix. Moreover, $\mathbf{u}_{vs2}$ is a nonlinear feedback term used to deal with the influence of model uncertainties for a guaranteed robust performance, which is satisfied the following two conditions

$$\begin{aligned} &1)\mathbf{e}(\mathbf{u}_{vs2} - \boldsymbol{\Psi}_k^T(\mathbf{q}, \dot{\mathbf{q}}, t)\tilde{\boldsymbol{\theta}} + \tilde{\mathbf{d}_k}) \leq \boldsymbol{\epsilon}_k \\ &2)\mathbf{e}\mathbf{u}_{vs2} \leq 0 \end{aligned} \tag{22}$$

where $\boldsymbol{\epsilon}_k$ is arbitrarily small parameter. The adaptation function (15) is chosen as

$$\boldsymbol{\eta} = \boldsymbol{\Psi}_k^T(\mathbf{q}, \dot{\mathbf{q}}, t)\mathbf{e} \tag{23}$$

Noting that the control input $\mathbf{v}_d$ contains virtual desired linear velocity v_{xd} and angular velocity $\omega_{\phi d}$ of the mobile robot. Thus, the desired angular velocity of each wheel can be derived as

$$\begin{aligned} &\omega_{di} = (v_{xd} - \omega_{\phi d} * w)/r, i = 1, 3 \\ &\omega_{di} = (v_{xd} + \omega_{\phi d} * w)/r, i = 2, 4 \end{aligned} \tag{24}$$

where ω_{di} is the desired wheel velocity.

Remark 1. *The desired wheel velocities* (24) *are not only used for the traditional kinematic controller design that will be compared with the proposed controller, but also adopted in the coordinated control later, Fig.3.*

D. The ARC Controller

A switching-function-like quantity is defined as

$$\mathbf{s} = \dot{\mathbf{e}} + \boldsymbol{\Lambda}\ \mathbf{e} \tag{25}$$

where $\boldsymbol{\Lambda} > 0$ represents a diagonal matrix. Choose a positive Lyapunov function

$$\mathbf{V}(t) = \frac{1}{2}\mathbf{s}^T\mathbf{M}_t\mathbf{s} \tag{26}$$

Differentiating equation.(26), the time derivative of $\mathbf{V}(t)$ can be described as

$$\begin{aligned} &\dot{\mathbf{V}} = \mathbf{s}^T[\mathbf{u}_t + \mathbf{d}_t - \mathbf{A}_t + \tilde{\boldsymbol{\Delta}}_t - \mathbf{C}_t\dot{\mathbf{e}} - \mathbf{B}_t\dot{\mathbf{e}} - \mathbf{M}_t\ddot{\mathbf{z}}_d \\ &-\mathbf{C}_t\dot{\mathbf{z}}_d - \mathbf{B}_t\dot{\mathbf{z}_d}] \end{aligned} \tag{27}$$

Furthermore, equation.(27) can be linearly parameterized as

$$\begin{aligned}&\mathbf{M}_t\ddot{\mathbf{z}}_d + \mathbf{C}_t\dot{\mathbf{z}}_d + \mathbf{B}_t\dot{\mathbf{z}}_d + \mathbf{C}_t\dot{\mathbf{e}} + \mathbf{B}_t\dot{\mathbf{e}} - \mathbf{d}_t \\ &+\mathbf{A}_t = -\boldsymbol{\Psi}(\mathbf{z}, \dot{\mathbf{z}}, \mathbf{t})\boldsymbol{\theta}\end{aligned} \tag{28}$$

where $\boldsymbol{\Psi} \in R^{2\times 8}$ matrix is a known functions. Thus, equation.(28) can be rewritten as

$$\dot{\mathbf{V}} = \mathbf{s}^T[\mathbf{u}_t + \boldsymbol{\Psi}(\mathbf{z}, \dot{\mathbf{z}}, \mathbf{t})\boldsymbol{\theta} + \tilde{\boldsymbol{\Delta}}] \tag{29}$$

Noting the equation (29), the virtual control input is chosen as

$$\mathbf{u}_d = \mathbf{T}^{-1}\mathbf{u}_t, \mathbf{u}_t = \mathbf{u}_a + \mathbf{u}_s, \mathbf{u}_a = -\boldsymbol{\Psi}(\mathbf{q}, \dot{\mathbf{q}}, t)\hat{\boldsymbol{\theta}} \tag{30}$$

where $\mathbf{u}_a$ is the adjustable model compensation to achieve a perfect tracking performance, and $\mathbf{u}_s$ represents a robust control law term. Substituting (30) into (29) result in

$$\dot{\mathbf{V}} = \mathbf{s}^T[\mathbf{u}_s - \boldsymbol{\Psi}(\mathbf{q}, \dot{\mathbf{q}}, t)\tilde{\boldsymbol{\theta}} + \tilde{\boldsymbol{\Delta}}] \tag{31}$$

The robust control function $\mathbf{u}_s$ consists of two terms

$$\mathbf{u}_s = \mathbf{u}_{s1} + \mathbf{u}_{s2}, \ \mathbf{u}_{s1} = -\mathbf{K}\mathbf{s} \tag{32}$$

where $\mathbf{u}_{s1}$ is a simple linear feedback term and $\mathbf{K}$ is a symmetric positive definite matrix. Moreover, $\mathbf{u}_{s2}$ is a nonlinear feedback term used to deal with the influence of model uncertainties for a guaranteed robust performance, which is satisfied the following two conditions

$$\begin{aligned}&1)\mathbf{s}(\mathbf{u}_{s2} - \boldsymbol{\Psi}^T(\mathbf{q}, \dot{\mathbf{q}}, t)\tilde{\boldsymbol{\theta}} + \tilde{\boldsymbol{\Delta}}) \leq \boldsymbol{\epsilon} \\ &2)\mathbf{s}\mathbf{u}_{s2} \leq 0\end{aligned} \tag{33}$$

where $\boldsymbol{\epsilon}$ is arbitrarily small . The smooth examples of $\mathbf{u}_{s2}$ satisfying (33) can be found [27].

E. Wheel torque allocation and coordinated control

The section introduce the wheel torque allocation algorithm and the wheel torque coordinate controller design. For the wheel torque allocation, the desired driving torques of each wheel is derived with the nominal vertical tire force. However, since the skid steer mobile robot is lack of suspension system and the various ground conditions, the driving torques from the driving torque allocation may cause the wheel slip and wheel velocity may become very large. To avoid this phenomenon, a novel hybrid coordinate control law is proposed.

The total virtual driving forces $\mathbf{u}_d$ given in equation(30) consists of the longitudinal driving force u_{xd} and the yaw moment $u_{\phi d}$. These virtual inputs from ARC controller are combined effort of each driving wheel. Therefore, the wheel torque allocation algorithm is designed to generate the wheel torque at each wheel based on the virtual inputs. Thus, a following cost function is chosen to achieve the desired wheel torque of each wheel.

$$J_{cost} = \sum_{i=1}^{4} W_i \frac{F_{xi}^2 + F_{yi}^2}{N_i^2} \tag{34}$$

where N_i is the nominal vertical tire force, which can be expressed in the following term

$$N_i = \tfrac{Mgl_r}{2(l_f+l_r)}, i = 1, 2, N_i = \tfrac{Mgl_f}{2(l_f+l_r)}, i = 3, 4 \tag{35}$$

The desired tire force have to satisfy the following constraints

$$\begin{aligned}u_{xd} &= F_{x1} + F_{x2} + F_{x3} + F_{x4} \\ u_{\phi d} &= -w_l F_{x1} + l_f F_{y1} + w_r F_{x2} + l_f F_{y12} \\ &\quad -w_l F_{x3} - l_r F_{y3} + w_r F_{x4} - l_r F_{y4}\end{aligned} \tag{36}$$

The lateral tire force $F_{yi}, i = 1, 2, 3, 4$ can be calculated[1]. Thus, the constraints can be rewritten as

$$\begin{aligned}u_{xd} &= F_{x1} + F_{x2} + F_{x3} + F_{x4} \\ M_d &= -wF_{x1} + wF_{x2} - wF_{x3} + wF_{x4}\end{aligned} \tag{37}$$

where $M_d = u_{\phi d} - l_f F_{y1} - l_f F_{y2} + l_r F_{y3} + l_r F_{y4}$. Substituting equations (37) into equation (34), the desired longitudinal tire torque $F_{xi}, i = 1, 2, 3, 4$ at each wheel can be obtained by lagrange multiplier. Thus, we can obtain following equation

$$\begin{aligned}\tfrac{\partial J}{\partial x_i} &= 2W_i \tfrac{x_i}{N_i^2} + \lambda_1 - w\lambda_2 = 0, i = 1, 2, 3, 4 \\ \tfrac{\partial J}{\partial \lambda_1} &= F_{x1} + F_{x2} + F_{x3} + F_{x4} = u_{xd} \\ \tfrac{\partial J}{\partial \lambda_2} &= -wF_{x1} + wF_{x2} - wF_{x3} + wF_{x4} = M_d\end{aligned} \tag{38}$$

where λ_i represents the lagrange multiplier. With the above equations(38), the desired force of each wheel F_{xi} then can be derived.

$$\tau_{ri1} = F_{xi}r + \hat{J}_{ri}\dot{\omega}_{di} + \hat{c}_{ri}\omega_{di} + \hat{f}_{ri} \tag{39}$$

where $\hat{J}_{ri}$ and $\hat{c}_{ri}$ are obtained from offline parameter estimation, ω_{di} is the desire wheel velocity from the kinematic controller(24).

However, since the 4 wheel-independently-driven mobile robot lack the suspension system, the wheel may lift from the ground. Thus, the above control input τ_{ri1} may cause the wheel velocity becoming very large. In this study, a hybrid coordinated feedback of the wheel slip is introduced to limit the wheel velocity. From the kinematic controller, the desired wheel velocity has been derived. Thus, the difference between actual wheel velocity and the desired wheel velocity is used to avoid the wheel velocity becoming too large.

$$\tau_{ri2} = k_{ri}e_{ri} \tag{40}$$

where $e_{si} = \omega_{ri} - \omega_{di}$. Therefore, the control input can be derived as

$$\tau_{ri} = \tau_{ri1} + \tau_{ri2} \tag{41}$$

Remark 2. *The proposed control law τ_{ri} is a kind of hybrid controller. The first term of control input τ_{ri1} is applied to generate the desired forces of each wheel. However, considering the actual mobile robot in lab lack of suspension system, the control input τ_{ri1} may lead to the wheel velocity become very large. To avoid this phenomenon, the second term τ_{ri2} is proposed. Therefore, a novel hybrid controller is determined.*

IV. Experimental Results

A. Experimental Setup

To verify the effectiveness of the proposed controller, a skid-steered mobile robot from Guozi Robot is set up in Zhejiang University. As shown in Fig.4, the laboratory has a four-wheel independently driven skid-steered mobile robot. The position and orientation was estimated from the odometry and gyroscope. For this robot, we have the following parameters used in controller design: $w = 0.25m$, $l_f = l_r = 0.2m$, $M = 120kg$, $J = 5kgm^2$, $r = 0.16m$.

This article has been accepted for publication in a future issue of this journal, but has not been fully edited. Content may change prior to final publication. Citation information: DOI 10.1109/ACCESS.2017.2754647, IEEE Access

Fig. 4. Skid steer mobile robot

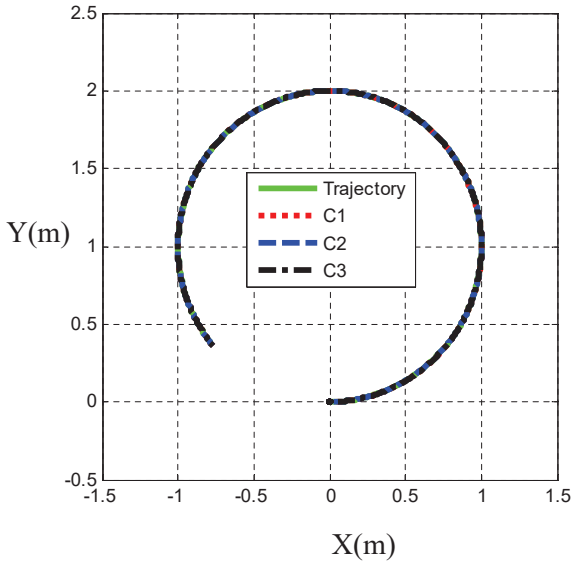

Fig. 5. Trajectory tracking performance of Set1

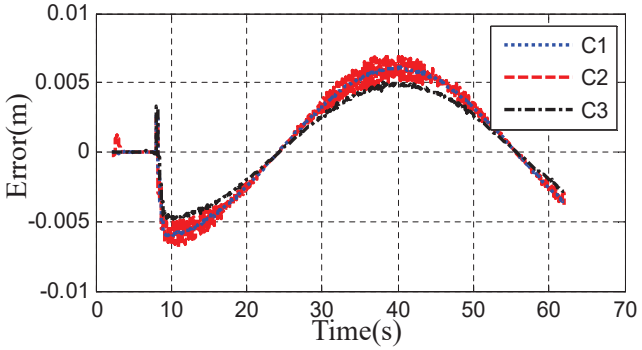

Fig. 6. Tracking error along x axis of Set1

B. Experimental Results

With a NI Compact-rio controller, the control algorithms are applied on the mobile robot. The control period is set as $Ts = 12$ ms. And the following controllers are compared to illustrate the performance of the proposed control algorithm.

C1) *Kinematic Control Algorithm*: This control method is the most used in actual equipment. From equation(24), the kinematic control law can be derived ω_{di}. The control parameters are properly as $K_k = [10, 10]$, and $\mathbf{\Gamma} = diag[25, 25, 0, 0, 0, 0, 0, 0, 0, 0]$. The desired velocities on each side are used as the reference velocity for the wheels which is tracked by a PID controller. With the PID controller, the poles closed-loop transfer functions are located at -20, such that the PID gains are derived as $k_i = 56, k_p = 5.6, k_d = 0$.

C2) *Proposed Control Law Without Compensation*: The proposed control law can be obtained from equation(39). The $\mathbf{\Lambda}$ is chosen as $\mathbf{\Lambda} = diag[5, 5]$. The robust control law is designed as $\mathbf{u}_s = -\mathbf{K}_2\mathbf{s}$ in the experiments, where $\mathbf{K}_2$ represents the combination of $\mathbf{u}_{s1}$ and $\mathbf{u}_{s2}$[19], [21]. With this simplified robust control term, the controller parameters are chosen as $\mathbf{K}_2 = [5.6, 5.6]^T$. The adaptation parameters are chosen as $\mathbf{\Gamma} = diag[0, 0, 1, 1, 0, 0, 56, 56, 0, 0]$. The wheel parameters used in Eq.(39) are estimated by standard parameter identification. The smooth functions S_f are chosen as$(2/\pi arctan(900\omega_{ri})$. And it is found that the parameters are $\hat{J}_{r1} = 0.14V/(m/s^2), \hat{c}_{r1} = 0.27V/(m/s), A_{f1} = 1.58$, $\hat{J}_{r2} = 0.14V/(m/s^2), \hat{c}_{r2} = 0.12V/(m/s), A_{f2} = 0.77$, $\hat{J}_{r3} = 0.14V/(m/s^2), \hat{c}_{r3} = 0.10V/(m/s), A_{f3} = 0.60$, $\hat{J}_{r4} = 0.14V/(m/s^2), \hat{c}_{r4} = 0.16V/(m/s), A_{f4} = 0.80$.

C3) *Proposed Control Law with compensation*: Compared with controller **C**2, a velocity compensation is added in this proposed control (41) so that the wheel velocity can be limited. The parameters are chosen as $k_{si} = 2, i = 1, 2, 3, 4$.

To illustrate the effectiveness of the proposed approach, the following test sets are performed.

Set 1: To test the control performance of the proposed algorithms, the mobile robot is applied to track a circle given by

$$\boldsymbol{\eta}_d = \begin{bmatrix} x_d \\ y_d \end{bmatrix} = \begin{bmatrix} cos(0.1t - \pi/2) \\ sin(0.1t - \pi/2) + 1 \end{bmatrix} \tag{42}$$

which the rotation velocity is $0.1rad/s$, and these experiments are tested on plain ground condition.

In the fist set of experiments, the tracking performance of the controller with circle trajectory on the plain ground is compared in Fig.5. As shown in Fig.6,7, it is found that the

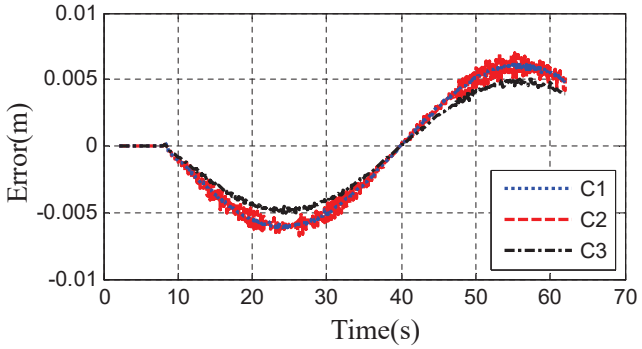

Fig. 7. Tracking error along y axis of Set1

This article has been accepted for publication in a future issue of this journal, but has not been fully edited. Content may change prior to final publication. Citation information: DOI 10.1109/ACCESS.2017.2754647, IEEE Access

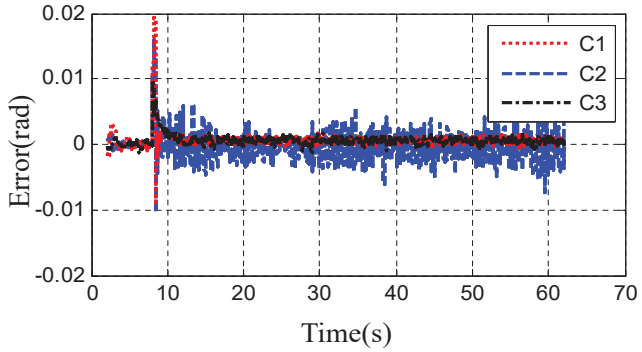

Fig. 8. Tracking error of the rotation angle of Set1

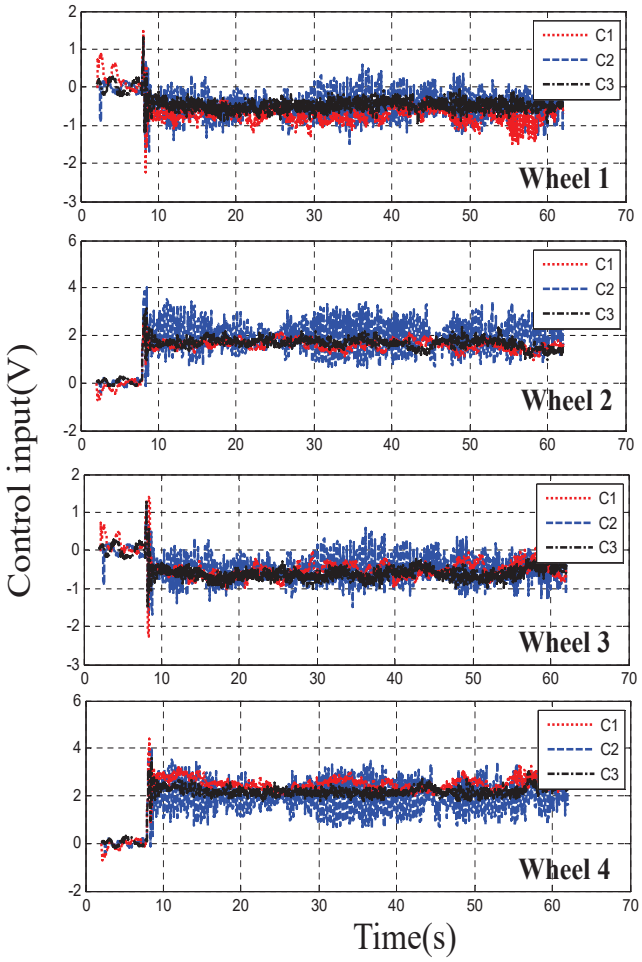

Fig. 9. Control inputs of Set1

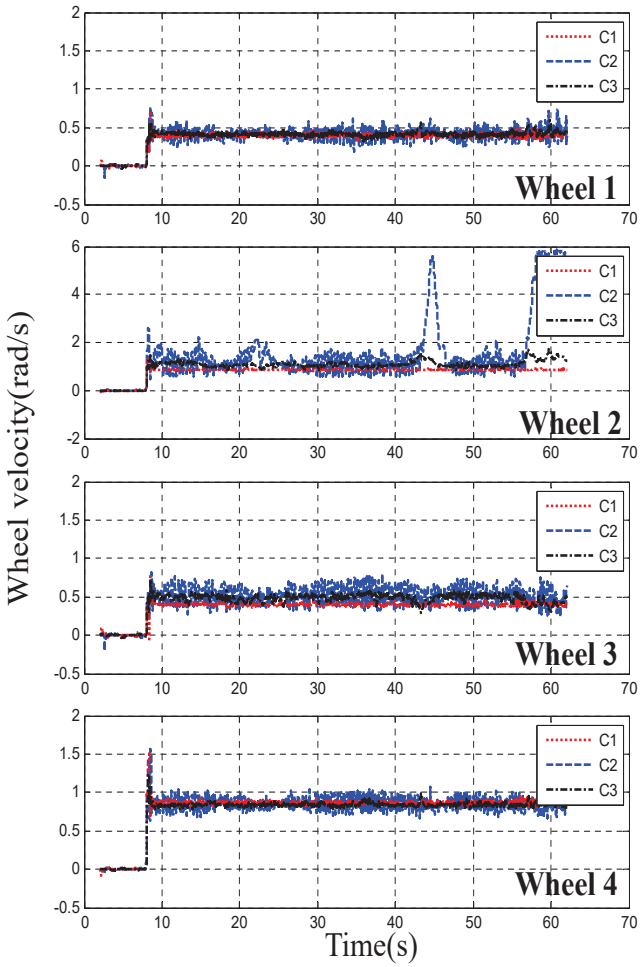

Fig. 10. Wheel velocities of Set1

proposed ARC controller with compensation achieve a smaller tracking error and a better performance than the other two. The angle tracking error is given in Fig.8, which also can reflect the chattering performance of the proposed controller. From this figure, the errors of **C**1 and **C**3 is obvious smaller than **C**2. From table. we find that **C**1 and **C**3 have similar angle tracking error, the ability of suppress the chattering phenomenon is difficult to identify. However, on the whole, the proposed controller **C**1 n can achieve a better tracking performance. As shown in Fig.9,10, the control inputs and wheel velocities are presented. With the controller **C**1, the wheel velocity on same side is same with each other, which is resulted from the PID controller to track the desired wheel velocities. However, the wheel velocity **C**2 will become very large when the wheel is lifted from ground. Compared with **C**1 and **C**2, the proposed controller achieve a integrated performance, whose velocities on the same side are not controlled to track the same desired velocity but also the wheel velocity can be limited.

***Set** 2*: From the actual application, when the mobile robot rotates on the rough terrain, the chattering phenomenon will happen with the traditional kinematic controller **C**1. To test the ability of proposed controller to suppress the chattering phenomenon, the mobile robot is applied to rotate on the rough terrain.

Furthermore, experiments *Set 2* are carried out to test the influence of the wheel/ground contact situation with the robot rotating on the rough ground. From the experiment results Fig.11,12,13, the capacity of suppressing the chattering phenomenon is presented. Since the controller **C**1 is a kinematic controller, the velocities on the same side are assumed to be same, which may cause that the frictions on the tire change very fast and motivate the chattering phenomenon. For **C**2, when the wheel is lifted from ground, the wheel velocity will become very large Fig.14, which result in the chattering

This article has been accepted for publication in a future issue of this journal, but has not been fully edited. Content may change prior to final publication. Citation information: DOI 10.1109/ACCESS.2017.2754647, IEEE Access

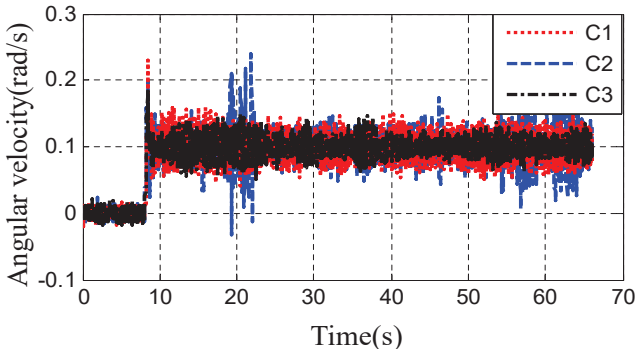

Fig. 11. Angular velocities of Set2

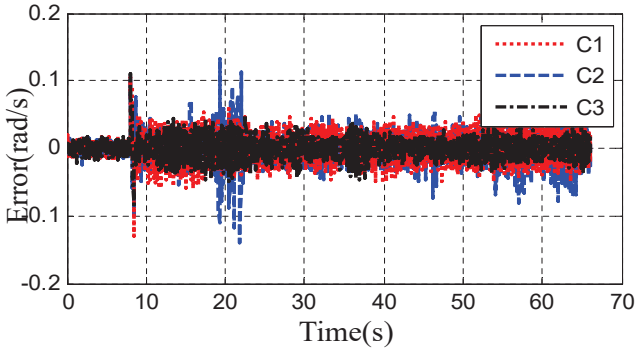

Fig. 12. Error of angular velocities in Set2

of robot. However, since the controller **C**3 considered these two factors, the integrated performance is achieved and the chattering phenomenon is well suppressed.

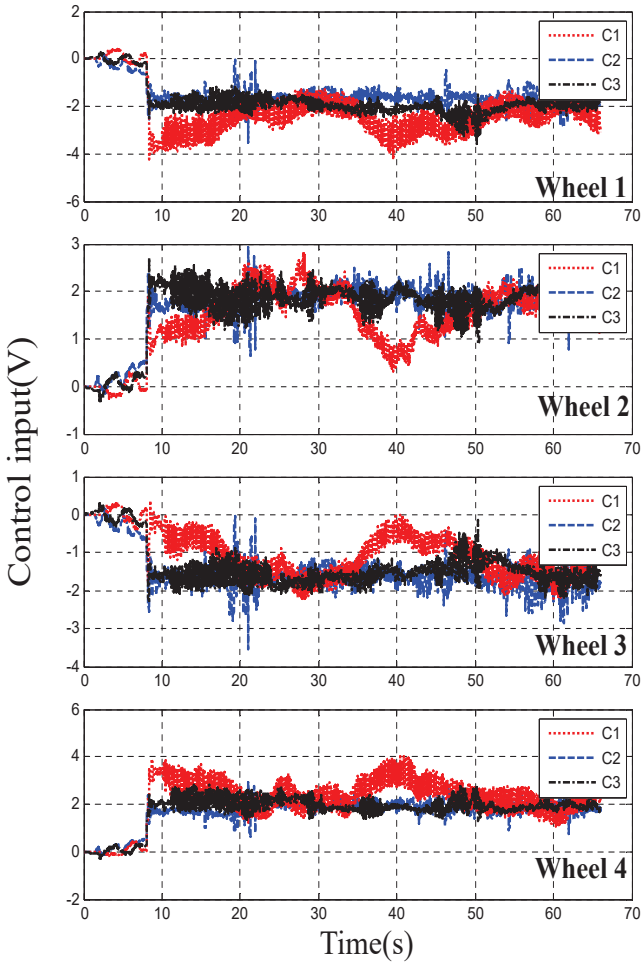

Fig. 13. Control inputs of Set2

V. Conclusion

In this paper, the coordinated control problem is investigated for the four-wheel independently driven skid steer mobile robots. A generalized nonlinear time-varying dynamic model is developed for controller design. Moreover, a two level adaptive robust control law integrated with control allocation technique is proposed for the skid steer mobile robot. In the high level, an adaptive robust control law is developed to achieve a good trajectory tracking control performance. In the low level, a torque allocation technique is developed for regulating driving torque of each motor. Meanwhile, to avoid the wheel velocity become too large when the tire is lifted from ground. A novel feedback of the wheel slip is proposed. Comparative simulations are carried out to verify the excellent performance of the proposed scheme. The experiment results suggest that, the proposed controller will achieve a good performance and adapt well with the ground condition .

References

[1] E. Mohammadpour and M. Naraghi, "Robust adaptive stabilization of skid steer wheeled mobile robots considering slipping effects," *Advanced Robotics*, vol. 25, no. 1-2, pp. 205–227, 2011.

[2] J. Yi, D. Song, J. Zhang, and Z. Goodwin, "Adaptive trajectory tracking control of skid-steered mobile robots," in *IEEE International Conference on Robotics and Automation*, 2007, pp. 2605–2610.

[3] J. Yi, H. Wang, J. Zhang, D. Song, S. Jayasuriya, and J. Liu, "Kinematic modeling and analysis of skid-steered mobile robots with applications to low-cost inertial-measurement-unit-based motion estimation," *Robotics, IEEE Transactions on*, vol. 25, no. 5, pp. 1087–1097, 2009.

[4] Z.-G. Hou, A.-M. Zou, L. Cheng, and M. Tan, "Adaptive control of an electrically driven nonholonomic mobile robot via backstepping and fuzzy approach," *IEEE Transactions on Control Systems Technology*, vol. 17, no. 4, pp. 803–815, 2009.

[5] J. Huang, C. Wen, W. Wang, and Z.-P. Jiang, "Adaptive output feedback tracking control of a nonholonomic mobile robot," *Automatica*, vol. 50, no. 3, pp. 821–831, 2014.

[6] T. Urakubo, K. Tsuchiya, and K. Tsujita, "Motion control of a two-wheeled mobile robot," *Advanced Robotics*, vol. 5, no. 7, pp. 711–728, 1999.

[7] J. C. Ryu and S. K. Agrawal, "Differential flatness-based robust control of mobile robots in the presence of slip," *International Journal of Robotics Research*, vol. 30, no. 4, pp. 463–475, 2011.

[8] W. Sun, S. Tang, H. Gao, and J. Zhao, "Two time-scale tracking control of nonholonomic wheeled mobile robots," *IEEE Transactions on Control Systems Technology*, vol. 24, no. 6, pp. 2059–2069, 2016.

[9] B. L. Chang and D. Wang, "Gps-based tracking control for a car-like wheeled mobile robot with skidding and slipping," *Mechatronics IEEE/ASME Transactions on*, vol. 13, no. 4, pp. 480–484, 2008.

[10] C. B. Low and D. Wang, "Gps-based path following control for a car-like wheeled mobile robot with skidding and slipping," *IEEE Transactions on Control Systems Technology*, vol. 16, no. 2, pp. 340–347, 2008.

[11] B. Li, Y. Fang, and X. Zhang, "Visual servo regulation of wheeled mobile robots with an uncalibrated onboard camera," *IEEE/ASME Transactions on Mechatronics*, vol. 21, no. 5, pp. 2330–2342, 2016.

[12] Z. Li, J. Deng, R. Lu, and Y. Xu, "Trajectory-tracking control of mobile robot systems incorporating neural-dynamic optimized model

This article has been accepted for publication in a future issue of this journal, but has not been fully edited. Content may change prior to final publication. Citation information: DOI 10.1109/ACCESS.2017.2754647, IEEE Access

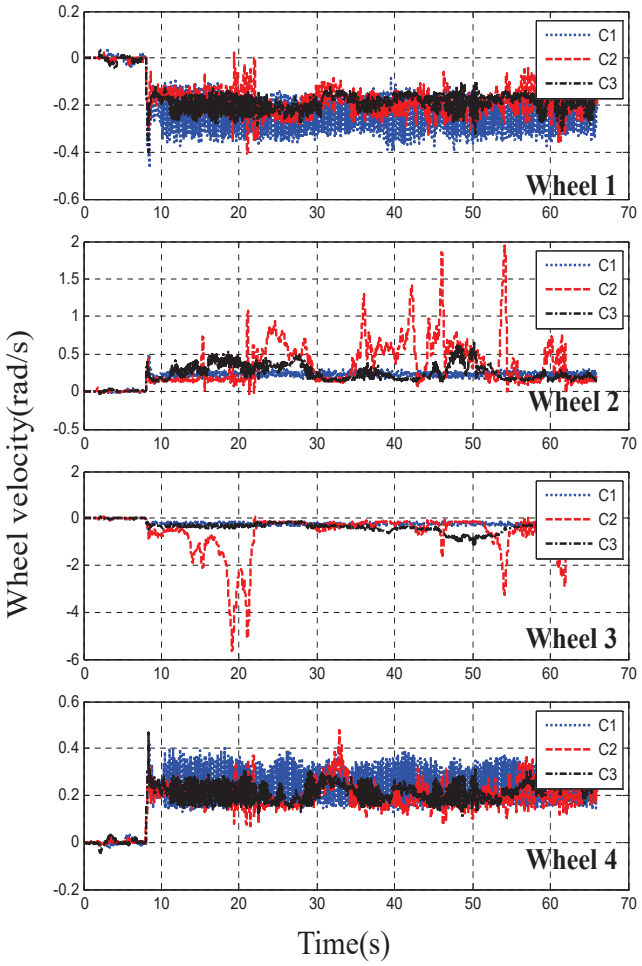

Fig. 14. Wheel velocities of Set2

predictive approach," *IEEE Transactions on Systems, Man, And cybernetics:systems*, vol. 46, no. 6, pp. 740–749, 2016.

[13] S. J. Yoo, "Adaptive tracking control for a class of wheeled mobile robots with unknown skidding and slipping," *Control Theory and Applications, IET*, vol. 4, no. 10, pp. 2109–2119, 2010.

[14] W. Sun, Y. Zhang, Y. Huang, H. Gao, and O. Kaynak, "Transient-performance-guaranteed robust adaptive control and its application to precision motion control systems," *IEEE Transactions on Industrial Electronics*, vol. 63, no. 10, pp. 6510–6518, 2016.

[15] Z. Feng and W. X. Zheng, "On extended dissipativity of discrete-time neural networks with time delay." *IEEE Transactions on Neural Networks & Learning Systems*, vol. 26, no. 12, pp. 3293–3300, 2015.

[16] Z. Feng and J. Lam, "Stability and dissipativity analysis of distributed delay cellular neural networks." *IEEE Transactions on Neural Networks*, vol. 22, no. 6, pp. 976–981, 2011.

[17] J. Yao, Z. Jiao, and D. Ma, "Extended-state-observer-based output feedback nonlinear robust control of hydraulic systems with backstepping," *IEEE Transactions on Industrial Electronics*, vol. 61, no. 61, pp. 6285–6293, 2014.

[18] J. Yao, Z. Jiao, D. Ma, and L. Yan, "High-accuracy tracking control of hydraulic rotary actuators with modeling uncertainties," *IEEE/ASME Transactions on Mechatronics*, vol. 19, no. 2, pp. 633–641, 2014.

[19] B. Yao and M. Tomizuka, "Adaptive robust control of siso nonlinear systems in a semi-strict feedback form," *Automatica*, vol. 33, no. 5, pp. 893–900, 1997.

[20] C. Hu, Z. Wang, Y. Zhu, M. Zhang, and H. Liu, "Performance-oriented precision larc tracking motion control of a magnetically levitated planar motor with comparative experiments," *IEEE Transactions on Industrial Electronics*, vol. 63, no. 9, pp. 5763–5773, 2016.

[21] Z. Chen, Y. Pan, and J. Gu, "Integrated adaptive robust control for multilateral teleoperation systems under arbitrary time delays," *International Journal of Robust & Nonlinear Control*, vol. 26, no. 12, pp. 2708–2728, 2016.

[22] Z. Chen, Y.-J. Pan, and J. Gu, "A novel adaptive robust control architecture for bilateral teleoperation systems under time-varying delays," *International Journal of Robust & Nonlinear Control*, vol. 25, no. 17, pp. 3349–3366, 2015.

[23] A. Mazur and M. Cholewiski, "Virtual force concept in steering mobile manipulators with skid-steering platform moving in unknown environment," *Journal of Intelligent and Robotic Systems*, vol. 77, no. 3-4, pp. 433–443, 2015.

[24] O. Elshazly, A. Abo-Ismail, H. S. Abbas, and Z. Zyada, "Skid steering mobile robot modeling and control," in *Control (CONTROL), 2014 UKACC International Conference on*. IEEE, Conference Proceedings, pp. 62–67.

[25] Y. Chen and J. Wang, "Adaptive energy-efficient control allocation for planar motion control of over-actuated electric ground vehicles," *Control Systems Technology, IEEE Transactions on*, vol. 22, no. 4, pp. 1362–1373, 2014.

[26] ——, "Design and experimental evaluations on energy efficient control allocation methods for overactuated electric vehicles: Longitudinal motion case," *IEEE/ASME Transactions on Mechatronics*, vol. 19, no. 2, pp. 538–548, 2014.

[27] B. Yao, F. Bu, J. Reedy, and G. T. C. Chiu, "Adaptive robust motion control of single-rod hydraulic actuators: Theory and experiments," *IEEE/ASME Transactions on Mechatronics*, vol. 5, no. 1, pp. 79–91, 2000.

[28] T. A. Johansen and T. I. Fossen, "Control allocationła survey ," *Automatica*, vol. 49, no. 5, pp. 1087–1103, 2013.

[29] H. Alwi and C. Edwards, "Fault tolerant control using sliding modes with on-line control allocation," *Automatica*, vol. 44, no. 7, pp. 1859–1866, 2008.

[30] J. Tjonnas and T. A. Johansen, "Stabilization of automotive vehicles using active steering and adaptive brake control allocation," *IEEE Transactions on Control Systems Technology*, vol. 18, no. 3, pp. 545–558, 2010.

[31] M. G. Feemster and J. M. Esposito, "Comprehensive framework for tracking control and thrust allocation for a highly overactuated autonomous surface vessel," *Journal of Field Robotics*, vol. 28, no. 1, pp. 80–100, 2011.

[32] E. J. RodrÍguez-Seda, C. Tang, M. W. Spong, Stipanovi, Du, and M. An, "Trajectory tracking with collision avoidance for nonholonomic vehicles with acceleration constraints and limited sensing," *International Journal of Robotics Research*, vol. 33, no. 12, pp. 1569–1592, 2014.

[33] C. Hu, B. Yao, and Q. Wang, "Coordinated adaptive robust contouring control of an industrial biaxial precision gantry with cogging force compensations," *Industrial Electronics, IEEE Transactions on*, vol. 57, no. 5, pp. 1746–1754, 2010.

[34] Z. Chen, B. Yao, and Q. Wang, "μ-synthesis-based adaptive robust control of linear motor driven stages with high-frequency dynamics: A case study," *IEEE/ASME Transactions on Mechatronics*, vol. 20, no. 3, pp. 1482–1490, 2015.

[35] ——, "Accurate motion control of linear motors with adaptive robust compensation of nonlinear electromagnetic field effect," *IEEE/ASME Transactions on Mechatronics*, vol. 18, no. 3, pp. 1122–1129, 2013.